REPORT DOCUMENTATION PAGE

Form Approved OMB No. 0704-0188

1. REPORT DATE *(DD-MM-YYYY)*	2. REPORT TYPE	3. DATES COVERED *(From – To)*
02-04-2004	Final Report	10 January 2003 - 21-Jun-04

4. TITLE AND SUBTITLE

Fast detection of high power microwave signals using asymmetrically shaped semiconductor structures

5a. CONTRACT NUMBER
FA8655-03-1-3021

5b. GRANT NUMBER

5c. PROGRAM ELEMENT NUMBER

6. AUTHOR(S)

Professor Steponas Asmontas

5d. PROJECT NUMBER

7. PERFORMING ORGANIZATION NAME(S) AND ADDRESS(ES)

Semiconductor Physics Institute
A.Gostauto 11
Vilnius 2600
Lithuania

8. PERFORMING ORGANIZATION REPORT NUMBER

N/A

9. SPONSORING/MONITORING AGENCY NAME(S) AND ADDRESS(ES)

EOARD
PSC 802 BOX 14
FPO 09499-0014

10. SPONSOR/MONITOR'S ACRONYM(S)

11. SPONSOR/MONITOR'S REPORT NUMBER(S)
SPC 03-4021

12. DISTRIBUTION/AVAILABILITY STATEMENT

Approved for public release; distribution is unlimited. (approval given by local Public Affairs Office)

13. SUPPLEMENTARY NOTES

14. ABSTRACT

This report results from a contract tasking Semiconductor Physics Institute as follows: The contractor will investigate methods of creating a fast detector of high power microwave radiation that can measure the amplitude of the pulses of nanoseconds duration in the order of 100 kW. The contractor's investigation will include:
1. Detection properties of asymmetrically shaped semiconductor structure, fabricated on the base of silicon single crystal;
2. Suitability of the device to detect high power microwave signals using asymmetrically shaped AlGaAs structures.
The contractor will deliver 12 asymmetrically shaped sensors to: Dr John Gaudet, AFRL/DE, Bldg 909, 3550 Aberdeen Ave SE, Kirtland AFB NM 87117-5776.

15. SUBJECT TERMS

EOARD, High Power Microwaves, High Power Microwave Sensors, Semiconductor materials

16. SECURITY CLASSIFICATION OF:			17. LIMITATION OF ABSTRACT	18. NUMBER OF PAGES	19a. NAME OF RESPONSIBLE PERSON
a. REPORT	b. ABSTRACT	c. THIS PAGE			MICHAEL KJ MILLIGAN, Lt Col, USAF
UNCLAS	UNCLAS	UNCLAS	UL	33	19b. TELEPHONE NUMBER *(Include area code)* +44 (0)20 7514 4955

Standard Form 298 (Rev. 8/98)
Prescribed by ANSI Std. Z39-18

AQ F04-11-1281

UNCLASSIFIED

EOARD Contractor Final Performance Report

European Office of Aerospace Research & Development

Fast detection of high power microwave signals using asymmetrically shaped semiconductor structures

Steponas Ašmontas and Algirdas Sužiedėlis

Award No. FA8655-03-1-3021

March 2004

PUSLAIDININKIŲ FIZIKOS INSTITUTAS
PFI

UNCLASSIFIED

Distribution A:

Approved for Public Release
Distribution is Unlimited

UNCLASSIFIED

EOARD Contractor Final Performance Report

Fast detection of high power microwave signals using asymmetrically shaped semiconductor structures

Steponas Ašmontas and Algirdas Sužiedėlis

Nonuniform Structures Laboratory
Semiconductor Physics Institute
Vilnius Lithuania

Prepared for EOARD
Under Award No. FA8655-03-1-3021

March 2004

Contents

Report documentation page (SF298) 3

Symbols, Abbreviations, and Acronyms 4

Summary 5

List of People Involved 6

Publications Stemming from the Research 7

Introduction 8

Theoretical approach 10

Samples and Experimental 14

Experimental Results 19

Conclusions 28

Recommendations 29

References 30

Acknowledgements 31

Clause Statements 32

Appendix A 33

Symbols, Abbreviations, and Acronyms

ASPD	- asymmetrically shaped planar diode
a	- width of ASPD
C	- electrical capacitance
d	- width of the narrowest part of ASPD
E_c	- critical electric field strength
EM	- electromagnetic
emf	- electromotive force
f	- frequency
f_{pulse}	- frequency of modulation
HCD	-detector on the basis of hot carrier effect
HPM	- high power microwaves
h	- structure thickness
h_{mesa}	- height of mesa
I-V	- current voltage
K	- factor indicating the amount of microwave power absorbed by diode
K_a	- (26÷37) GHz frequency range
L	- length of diode's part from the "neck" up to metallic contacts
l-h	- semiconductor junction with low and high doping level
MW	- microwaves
n	- electron concentration
P	- microwave power absorbed by diode
P_i	- incident microwave power
P_{imax}	- dynamic range upper limit
p	- hole concentration
R	- electrical resistance
R_s	- surface resistivity
R_{s0}	- geometrical resistance of ASPD
SI	- semiinsulating (substrate)
S_i	- voltage sensitivity with respect to incident microwave power
S_a	- voltage sensitivity with respect to absorbed microwave power
s	- power dependence index of electron pulse relaxation time on energy
T	- temperature
THz	- terahertz (frequency)
U_d	- detected voltage
X	- (8÷12) GHz frequency range
x	- mole fraction of AlAs
x_j	- diffusion depth of impurity
α	- widening angle of ASPD
μ_0	- low field electron mobility
ρ	- electrical resistivity
ρ^n	- electrical resistivity of n-region
τ	- time constant
τ_E	- electron energy relaxation time
τ_M^n	- Maxwell relaxation time in n region
τ_p	- electron pulse relaxation time
ω	- angular frequency of microwave radiation

Summary

Theoretical and experimental research of asymmetrically shaped planar semiconductor detectors was performed with intent to establish their possibility to detect fast microwave signals of high power. Silicon structures both barrier-less and with *l-h*-potential barrier were investigated; additionally, barrier-less detectors on the base of *n*-type AlGaAs layers with various AlAs mole fraction x values (0.1÷0.4) were explored. The best candidate for the highest operational speed (several nanoseconds) turned to be made of high resistivity *p*-type silicon with potential barrier inlaid. Calculations (100 kW) and experiment (up to 40 kW) showed that the widest dynamic range also had the detector of the same material and structure but of low resistivity; this was realized through effective shunting of microwave currents by the semiconductor substrate and higher value of critical electric field strength for *p*-type silicon compared to that for *n*-silicon. In contrast to the theoretical predictions, the highest upper dynamic range limit (10 kW) was achieved for the detectors made of AlGaAs with $x = 0.31$; unfortunately, lower x values were accompanied by electrical charge inhomogeneities, while the higher ones caused polycrystallization of the layers grown by liquid phase epitaxy. On the basis of the achieved results recommendations to overcome the encountered difficulties were proposed.

List of People Involved

Steponas Ašmontas, Prof. (principal)

Algirdas Sužiedėlis, Assoc. Prof. (research, analysis and writing)

Jonas Gradauskas, Assoc. Prof. (editor)

Jurgis Kundrotas, Dr. Habil. (photoluminescence research)

Aldis Šilėnas, PhD (liquid phase epitaxy growth)

Andžej Lučun, PhD student (MW research)

Valerij Petkun, Master sudent (MW research)

Publications Stemming from the Research

- HIGH POWER MICROWAVE DETECTION IN ASYMMETRICALLY SHAPED SEMICONDUCTOR STRUCTURES ON SEMICONDUCTOR SUBSTRATE
  S.Ašmontas, J.Gradauskas, V.Petkun, and A.Sužiedėlis
  Lithuanan Journal of Physics, Vol. 44, No. 5, 2003.

- HIGH POWER MICROVAVE DETECTION IN ASYMMETRICALLY SHAPED n-$Al_xGa_{1-x}As$ STRUCTURES
  S.Ašmontas, J.Gradauskas, J.Kundrotas, A.Lučun, V.Petkun,
  A.Šilėnas, and A.Sužiedėlis
  Theses for 12th Int. Symposium on Ultrafast Phenomena in Semiconductors (12 UFPS, Vilnius, Lithuania, 22-25 Aug 2004). Material of presentation will be published in *Acta Physica Polonica.*

Introduction

Recent interests in high power microwaves (HPM) is stipulated by the need to detect short pulses of HPM in electronic countermeasure systems. The variety of technique of microwave (MW) generation opens a wide spectrum of features of the generated signals. Thus, HPM detectors must meet the requirements of the specific set of parameters enabling to detect and measure successfully high power and short pulses of the electromagnetic (EM) radiation in a wide frequency range. Reliability, high operational speed, wide frequency band of operation as well as non-sophisticated fabrication and service are the main features of such a detector. Table A1 in Appendix A demonstrates various principles of EM radiation detection, which can be used to measure high power of MWs. Each of the principles has its positive features as well as its weak points.

This project is subjected to the method of hot carrier thermo electromotive force (*emf*) for the microwave signal detection [1]. Frequency limit of operation of such detectors (or "hot carrier detector" - HCD) is set by electron momentum relaxation time, which in the case of commonly used semiconductors, such as Si or GaAs, is extended to terahertz frequency range. Reliability, simplicity of fabrication and convenience in maintenance are additional positive features of the HCD. Immunity against overload lies in the volumetric character of the thermoelectric effect of hot carriers, as distinct from Schottky detectors where the detection takes place on the surface of semiconductor. Fabrication of the HCD is a simple process consisting of usual technological processing steps such as oxidation, optical lithography, thermal diffusion and metallisation. The simplicity of operation of the HCD lies in the direct detection principle, i.e. the induced *emf* is measured over the ends of the sample without additional electrical biasing of the diode. Linear character of current voltage (I-V) characteristic determines weak dependence of the measured voltage on harmonics of microwave signal.

Investigation of the HCD with the aim to extend the dynamic range of the detector was performed under former EOARD grant [2]. The study of asymmetrically shaped microwave diodes on various semiconductor substrates revealed the possibility to measure the power of the microsecond microwave pulses up to the value of 8 kW. The main conclusion of this research work [2] was that the upper limit of dynamic range of the asymmetrically shaped diodes' operation was determined by the shunting properties of the substrate. Unexpected outcome of the investigation was the finding that the range limit could be raised if the asymmetrically shaped semiconductor structure were shunted by the subjacent semiconductor substrate of the same type of electrical conductivity.

That is why, during the current project we investigated the detection properties of the asymmetrically shaped semiconductor structures fabricated on the base of silicon single crystal. We predicted not only the increase of the dynamic range of the operation of these diodes but also the increase of the operational speed of the diodes due to the decrease of their electrical resistance. Variation of the thickness of the shunting semiconductor substrate would enable flexible change of the value of the total electrical resistance of the microwave diode. In addition, the use of a single crystal substrate simplifies the fabrication process of the diodes and, thus, lowers their cost.

The intention to increase both the voltage sensitivity and the operational speed of the planar asymmetrically shaped microwave diodes has brought us to the idea to use a semiconductor with higher electron mobility. Microwave diodes fabricated on the base of n-GaAs revealed themselves as more sensitive and faster detectors having wider dynamic range of operation than those fabricated from silicon [1]. Investigations of microwave detection features of whisker-contacted GaAs/AlGaAs heterojunctions showed crucial influence of intervalley electromotive force on the detected voltage [3]. The voltage sensitivity of the heterojunction diode in comparison with that of the homojunction diode was by two orders of magnitude higher, what we explained by the rise of intervalley *emf* appearing in the heterojunction along with the hot carrier thermo-*emf* and, as a result, considerably increasing the value of the detected signal. Another attractive feature of GaAs/AlGaAs heterojunction microwave diodes was the inversion of polarity of the detected voltage, what we associated with the origination of a negative differential resistance in the semiconductor due to the Gunn effect [3]. The latter property of the diode could be successfully used in the protection circuits of electronics against powerful microwave radiation. Therefore another part of this project is devoted to the investigation of planar microwave diodes on the base of AlGaAs ternary semiconductors. As a result of our research we expected to have sensitive, fast and burn-out resistant microwave diodes for HPM application.

Theoretical estimations of the detection properties of asymmetrically shaped planar diode (ASPD) on a single-crystal substrate of the same material were done in the Performance Report of the Project [4]. High electrical resistivity *p*-type silicon as well as *n*-type $Al_xGa_{1-x}As$ with AlAs mole fraction x exceeding 0.375 revealed themselves to be mostly preferable semiconductors for broadband detection of HPM. First experimental investigations of the ASPD on the base of n-n^+ junction and on barrier-less *n*-type semiconductor structure opened the possibility to measure power of the pulsed microwave radiation up to several kW. Independence of the detected signal on frequency was observed from X- to K_a- frequency ranges. The detected voltage was insensitive to the orientation of the ASPD with respect to the direction of incident MW power in a waveguide.

The second stage of the Project was assigned to the experimental study of high power microwave detection using *n*-Si ASPD with additionally shunting substrate doped into the outer surface of it. Also, the detection on asymmetrically shaped p-p^+ Si junction having various electrical resistivities was under the investigation. Experimental results of microwave detection on the barrier-less asymmetrically shaped diodes on the base of ternary semiconductor $Al_xGa_{1-x}As$ with various AlAs mole fractions are presented in the Final Report as well.

Theoretical approach

Phenomenological analysis of charge carrier transport in an asymmetrically shaped diode with n-n^+ junction gives the dependence of voltage sensitivity of the detector on the frequency of microwave electric field [1]:

$$S_i = \frac{U_d}{P_i} = \frac{\mu_0 (\rho^n)^2}{3h^2 d^2 R_{s0}} KN(\omega, \tau_p, \tau_E, \tau_M^n), \quad (1)$$

where U_d denotes the detected voltage, P_i is the incident microwave power in a waveguide, μ_0 is low field electron mobility, ρ^n stands for the resistivity of n-region of the ASPD, h is the thickness of the structure; d denotes the width of the semiconductor structure in the narrowest part ("neck's" width). The diode view can be seen in **Figure 4,** section "Samples and Experimental". R_{s0} is the geometrical resistance of the detector:

$$R_{s0} = \frac{\rho^n}{2h \tan\alpha} \ln(1 + a/d), \quad (2)$$

where α is the widening angle of the n-layer, a denotes the width of the semiconductor structure in its widest part. The factor N in Eq. (1) depends on electron pulse and energy relaxation times, τ_p and τ_E, as well as on Maxwell relaxation time τ_M^n in n region and defines the dependence of the voltage sensitivity on angular frequency ω of microwave radiation:

$$N = \frac{1}{1+(\omega\tau_p)^2} \frac{1+(\omega\tau_M^n)^2}{(\omega\tau_M^n)^2} \left\{ \tau_E \left[1 + \frac{s^2}{1+(\omega\tau_E)^2} \right] \ln\left[1+(\omega\tau_M^n)^2\right] + \right.$$
$$\left. + \tau_M^n \left[\frac{3}{2} - \frac{s(1-s)(\omega\tau_E)^2}{1+(\omega\tau_E)^2} \right] \left[\frac{1}{\omega\tau_M^n} \arctan \omega\tau_M^n - \frac{1}{1+(\omega\tau_M^n)^2} \right] \right\} + \quad (3)$$
$$+ \frac{s(1-s)\tau_E}{1+(\omega\tau_E)^2} \frac{1}{1+(\omega\tau_p)^2},$$

here s denotes the index of power dependence of electron pulse relaxation time on energy ($\tau_p \sim E^s$). The factor K in Eq. (1) can be found experimentally and it expresses the amount of the microwave power P absorbed by the diode:

$$K = P / P_i. \quad (4)$$

Phenomenological expression for the voltage sensitivity of a barrier-less asymmetrically shaped planar diode is not derived yet. Still numerical solution of electron transport equations can be used to find electron and electric field distributions at the "neck" of the semiconductor structure depending on the polarity of applied voltage. As a result, the asymmetry of I-V characteristic of the barrier-less ASPD was demonstrated and it revealed the possibility to detect microwave radiation: a bigradient *emf* arose over the ends of the diode [2]. The geometrical resistance of the barrier-less ASPD diode is expressed as follows:

$$R_{s0} = \frac{\rho^n}{2h} \left[\frac{1}{\tan\alpha_1} \ln\left(1 + \frac{2L_1}{d} \tan\alpha_2\right) + \frac{1}{\tan\alpha_2} \ln\left(1 + \frac{2L_2}{d} \tan\alpha_2\right) \right], \quad (5)$$

Figure 1. Frequency dependence of voltage sensitivity calculated with respect to absorbed microwave power for the ASPD (*a*) with *l-h* junction on silicon single-crystals, and (*b*) on AlGaAs epitaxial layers.

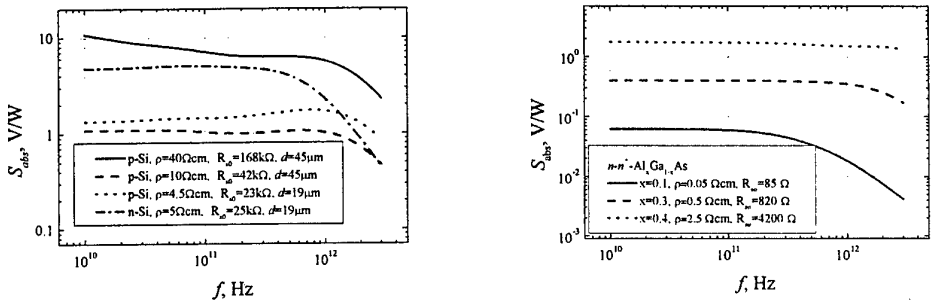

a) ***b)***

where α_1 and α_2 denote the widening angles of the left and the right parts of the semiconductor structure, respectively, while L_1 and L_2 stand for the length of the left and the right parts of the diode measured from the "neck" up to the metallic contacts.

Frequency dependences of the calculated voltage sensitivity of the asymmetrically shaped semiconductor structures with *l-h* junctions are presented in **Figure 1.** The sensitivities were calculated by formula (1) taking into account the value of the factor $K = 1$, i.e. the presented dependences refer to the voltage sensitivity correspondent to the absorbed microwave power (it is hard to evaluate theoretically the exact portion of the power absorbed by the microwave diode in a waveguide). The calculations were performed for the semiconductor material that was chosen for the fabrication of the ASPD (see **Figure 1, *a***): *p*-type Si with electrical resistivity of 4.5, 10, and 40 Ω·cm and *n*-type Si with $\rho = 5$ Ω·cm. The depth of the etched mesa was h =5 μm, the width of the diode a = 3 mm, and the widening angle of *n* region was $\alpha_1 = 45°$. The width of the "neck" of the structure d was taken either 45 μm (for *p*-type Si with $\rho = 10$ Ω·cm and 40 Ω·cm), or 19 μm (for *p*-type Si with $\rho = 4.5$ Ω·cm and *n*-type Si with $\rho = 5$ Ω·cm). In the case of $Al_xGa_{1-x}As$ semiconductor (**Figure 1, *b***), the calculations of the voltage sensitivity were performed for the values of AlAs mole fraction x equal to 0.1, 0.3, and 0.4. Now, the depth of mesa structure was h =20 μm, and the width of the "neck" was 45 μm. It is worth to note that the values of the electrical resistances given in **Figure 1** were calculated for the ASPD without a shunting semiconductor substrate.

Non-monotonic character of the frequency dependence of the voltage sensitivity up to terahertz (THz) frequency range is due to competitive mechanisms of microwave detection, such as: *i*) hot carrier electromotive force arising on *l-h* junction; and *ii*) rectification of microwave currents on charge non-uniformities. Dynamics of the hot carrier *emf* is determined by the electron energy relaxation time, while the microwave current rectification is conditioned by the Maxwell relaxation time. When the electron relaxation time exceeds the Maxwell one, then the hot carrier electromotive force dominates in the detected voltage and, *vice versus*, when the Maxwell relaxation time is longer than the electron relaxation time, then the

Figure 2. Theoretical dependences of the upper dynamic range limit of asymmetrically shaped silicon *l-h* junction (*a*) and barrier-less ASPD (*b*) on the depth of etched mesa

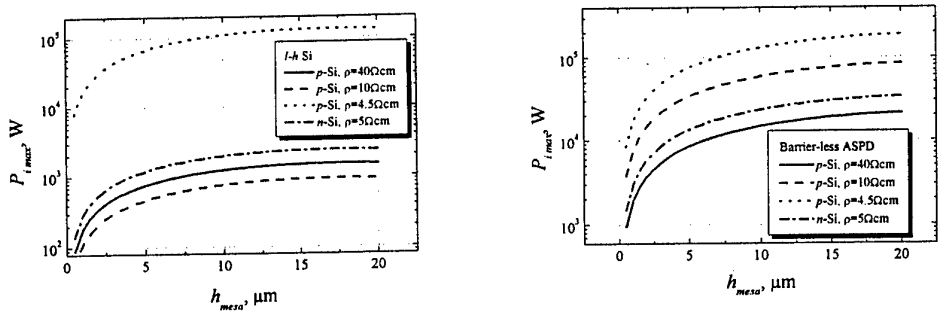

a) *b)*

microwave current rectification is leading. The decay of the detected voltage in THz frequency range is determined by the electron pulse relaxation time which, in its turn, depends on a semiconductor material: the shorter the time the wider plateau-like frequency dependence of the detected voltage. According to the results of calculation, the best candidates for wide frequency band application could be the ASPDs fabricated on the base of low resistivity *p*-type silicon, and the $Al_xGa_{1-x}As$ asymmetrically shaped structures with high value of AlAs mole fraction *x*.

Upper limit of the dynamic range of the ASPD is determined by the geometry of the diode and can be evaluated from formula:

$$P_{i\max} = \frac{E_c^2 d^2 h^2 R_{s0}}{\sqrt{2} K \rho^2}, \tag{6}$$

where E_c is critical electric field strength at which the dependence of charge carrier drift velocity on electric field deviates from the linear law. The value of E_c depends on the type of electrical conductivity of semiconductor as well as on the orientation of electric field vector with respect to crystallographic direction. Critical electric field strength values for semiconductors used for fabrication of the ASPDs are presented in Table 1.

Table 1. Values of critical electric field strength E_c for various semiconductors (taken from [4]).

Material	*n*-Si<100>	*p*-Si<100>	$Al_xGa_{1-x}As$		
			$x = 0.1$	$x = 0.3$	$x = 0.4$
E_c, kV/cm	2.0	4.5	1.5	3.0	4.5

Calculated dependences of the upper limit of dynamic range on the height of asymmetrically shaped semiconductor mesas are shown in **Figure 2**. The width of the "neck" of the ASPD was taken equal to 45 μm, and the values of the factor *K* were obtained from the comparison of experimental results of the voltage sensitivity with the theoretical one calculated according to Eq. (1). Higher upper limit of the dynamic range is expected for the ASPD fabricated on the base of low resistivity *p*-type silicon

($\rho = 4.5\ \Omega\cdot$cm). Moreover, the barrier-less microwave diodes must have wider dynamic range compared with that of the ASPD with *l-h* junction, as can be seen from **Figure 2**. This predication follows from Eq. (6): the P_{imax} is directly proportional to the electrical resistance of the asymmetrically shaped semiconductor structure, and the value of the resistance is higher in the case of barrier-less diode, as it follows from analysis of the formulae (2) and (5).

Figure 3.Theoretical dependences of the upper dynamic range limit of asymmetrically shaped AlGaAs ASPD on the depth of etched mesa

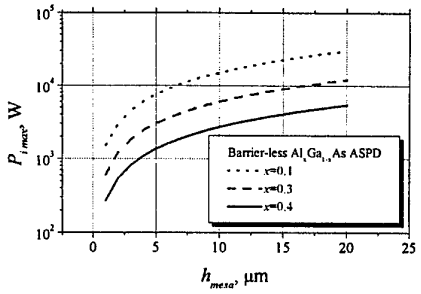

Theoretical evaluation of the upper dynamic limit of the ASPD on the base of $Al_xGa_{1-x}As$ epitaxial layer is summarized in **Figure 3**. More favorable candidates to measure higher values of microwave power seem to be the diodes with lower value of AlAs mole fraction x. The reason of this in our case lies in higher electrical conductivity of the semiconductor with lower x value (see inset in **Figure 1, *b***), and the higher value of the electric field strength E_c in the case of higher x values does not precede the weight of the electrical resistivity of semiconductor according to Eq. (6).

Samples and Experimental

Asymmetrically shaped planar diodes were fabricated on the base of two different semiconductor materials: on *n*-type and *p*-type single crystal silicon wafers, as well as on GaAs/AlGaAs epitaxial structures. The electrical resistivity ρ of *n*-Si was equal 7.5 Ω·cm, while that of *p*-Si was taken to be 4.5, 10.0, and 40.0 Ω·cm. The plane of the wafer of *p*-type silicon with ρ = 10 Ω·cm was oriented in (111) direction, while the planes of all the other silicon wafers were oriented in (100) direction. Epitaxial structures for the ASPD on the base of $Al_xGa_{1-x}As$ were grown by liquid phase epitaxy method on a semiinsulating substrate of GaAs oriented in (110) direction. The thickness of the grown *n*-$Al_xGa_{1-x}As$ layer was 20 μm, and mole fraction of AlAs, *x*, was taken to be equal 0.1, 0.3, and 0.4. Room temperature electron concentration and electron mobility values of the grown *n*-$Al_xGa_{1-x}As$ layers are given in Table 2. The calculated values of electrical resistivity of these layers are also presented in Table 2.

Table 2. Electrical parameters of epitaxial *n*-$Al_xGa_{1-x}As$ layers.

Mole fraction of AlAs, *x*	Electron concentration *n*, cm^{-3}	Electron mobility μ, $cm^2 \cdot V^{-1} \cdot s^{-1}$	Electrical resistivity ρ, Ω·cm
0.19	3×10^{16}	4020	0.05
0.23	7×10^{15}	1800	0.5
0.31	4×10^{15}	620	2.5

Schematic view of the asymmetrically shaped planar diodes fabricated on the base of silicon single-crystals is presented in Figure 4. Two types of silicon ASPDs were fabricated: *i*) the planar diode with asymmetrically shaped *l-h* (n-n^+ either p-p^+)

Figure 4. Schematic view of ASPDs on the base of single-crystal silicon: *a*) diode with asymmetrically shaped *l-h* junction; *b*) barrier-less diode.

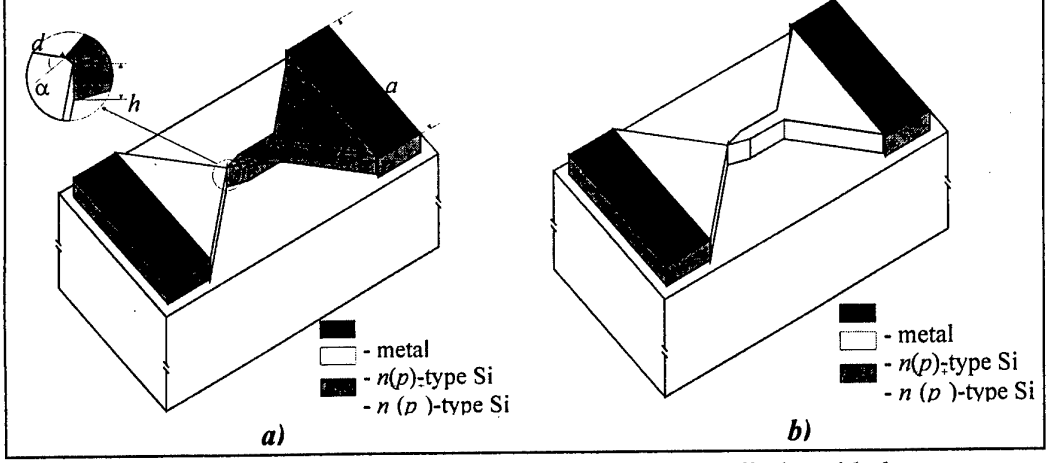

junction (is depicted in **Figure 4, *a***); and ***ii***) barrier-less diode with homogeneous asymmetrically shaped semiconductor structure (**Figure 4, *b***). Basic geometrical parameters of the silicon diodes were the following: the width *d* of the "neck" varied

Figure 5. Schematic view of ASPD on the base of AlGaAs epitaxial structure: *a*) diode with deep mesa; *b*) diode with shallow mesa.

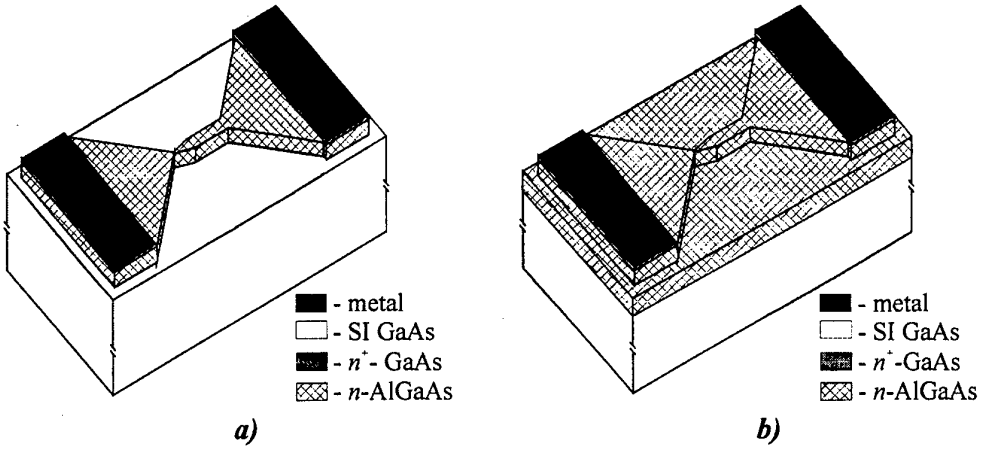

in the range of (20÷100) μm; the height h_{mesa} of the etched mesa was in the range of (5÷12) μm; the width of the diodes a was 3000 μm; and the widening angle α of n-region was equal to 45°. The shunting pad of the diodes had a double mission. First of all, it served as a protection of the "neck" by keeping out high power microwave signals of passing through it. This trick enabled us to increase the upper limit of dynamic range of the microwave diode. Another function of the shunting pad was to vary the value of the electrical resistance of the diode: by changing the thickness of the semiconductor wafer it was possible to reduce the electrical resistance of the diode what, in its turn, increased its operational speed. This was especially important in the case of the barrier-less diode, since the resistance of the asymmetrically configured semiconductor structure was much higher than that of the semiconductor substrate.

Two types of asymmetrically shaped barrier-less planar diodes were designed on the base of epitaxial AlGaAs layer: ***i***) planar diodes with deep asymmetrically shaped AlGaAs mesa formed onto semiinsulating GaAs, as shown in **Figure 5, *a*;** and ***ii***) diodes with shallow mesa (see **Figure 5, *b***). The second type of the ASPD was designed to extend the dynamic range of the microwave diodes and to increase their operational speed. Geometrical parameters of the "neck" of these ASPDs were the following: d = (20÷50) μm in both cases; h_{mesa} = (10÷15) μm in the case of the shallow mesa, and h_{mesa} = 25 μm for the deep mesa diodes.

Figure 6 presents the steps of fabrication process of the asymmetrically shaped planar microwave silicon diode with n-n^+ junction. The top view of the diode is shown in **Figure 6, *a*,** while the cross-section of the finished ASPD is depicted in **Figure 6, *g***. Thermal oxidation process of polished Si wafer was preceded by cleaning in acetone and chemical treatment in $H_2O : H_2O_2 : NH_4OH$ = 5:1:1 solution. Thermal oxidation of the wafer surfaces was performed at T = 1050°C in water vapor atmosphere. The thickness of the grown SiO_2 was 0.5 μm. First photolithography step was made to open the windows in SiO_2 for thermal diffusion (**Figure 6, *b***). The SiO_2 film was then removed from the flip-side of the wafer, thus making this side open for phosphorus doping also. The diffusion of phosphorus was made in two stages (**Figure 6, *c***). The first stage was performed at T = 950°C; as a result, the diffusion depth x_j = 0.3 μm

Figure 6. Fabrication process of ASPD on the base of *n*-type Si with *l-h* junction

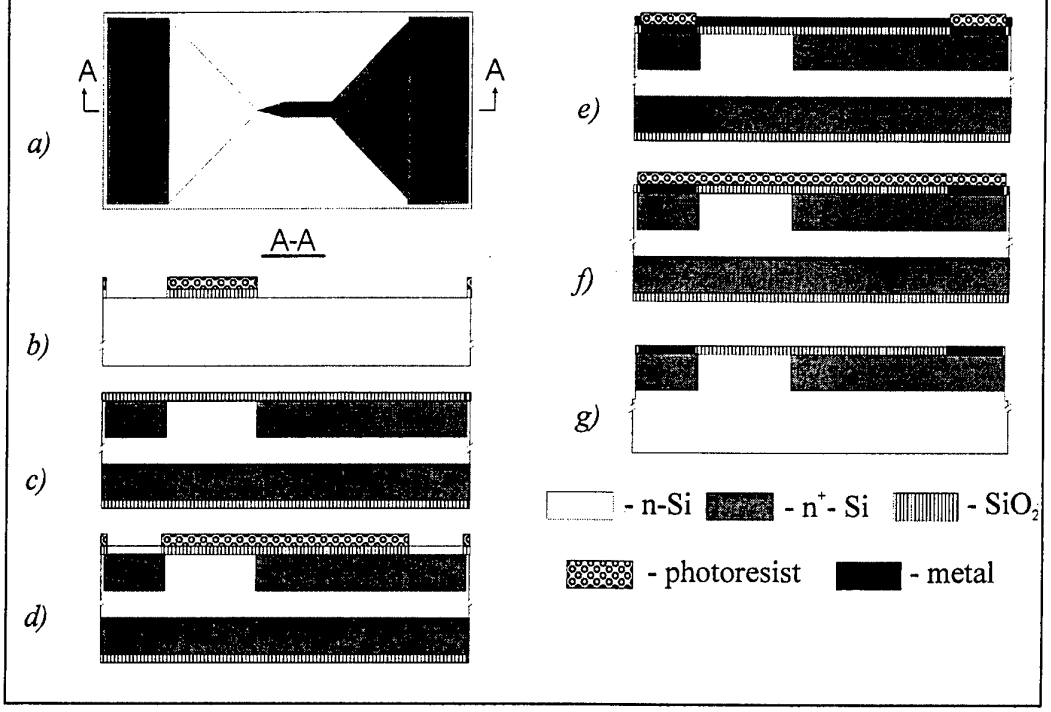

and the surface resistivity of the layer $R_s = 8\Omega/\square$ were achieved. In order to ensure a condition of finite source of phosphorus during the second stage of the diffusion, the phosphorus-silicon glass was removed from the diffused regions by wet chemical etching. The second stage of the phosphorus diffusion was performed at $T = 1150°C$ in water vapor and oxygen atmosphere; as a result, the diffusion depth was achieved $x_j = 5.0$ μm and the surface resistivity of the diffusion layer was $R_s = 3\Omega/\square$. SiO_2 grown during the second stage reached the thickness of ~ 0.5 μm. The second photolithography step was performed to open the windows in the oxide film for the metal contacts of the ASPD (**Figure 6, *d***). Aluminum film of 1 μm thickness was evaporated thermally as a contact layer. The third photolithography step was performed to form aluminum patterns of the microwave diode (**Figure 6, *e***). The metal contacts were annealed at $T = 450°C$ in argon atmosphere for 10 minutes. Mesa topology of the asymmetrically shaped semiconductor structures was patterned after the forth photolithography step (**Figure 6, *f***) using wet etching technique in $HNO_3 : HF : CH_3COOH = 40:1:1$ solution.(**Figure 6, *g***).

Processing of ASPD on the base of *p*-type Si was similar to the fabrication process described above. The main difference lay in the sequence of the technological steps. In this case mesa etching of the asymmetrically shaped semiconductor structure preceded metal contacts formation on the diode. This facilitated the deep mesa formation in the ASPD. As a doping impurity boron was used. During the first two stages of boron diffusion $x_j = 3.5$ μm and $R_s = 35\ \Omega/\square$ were achieved. Then the additional boron diffusion was performed for supplementary doping of the surface which had been depleted after the second stage: now boron was diffused into the depth of $x_j = 0.5$ μm making the surface resistivity $R_s = 40\ \Omega/\square$. Metallization of the

Figure 7. Fabrication process of barrier-less ASPD on the base of *n*-AlGaAs epitaxial layer

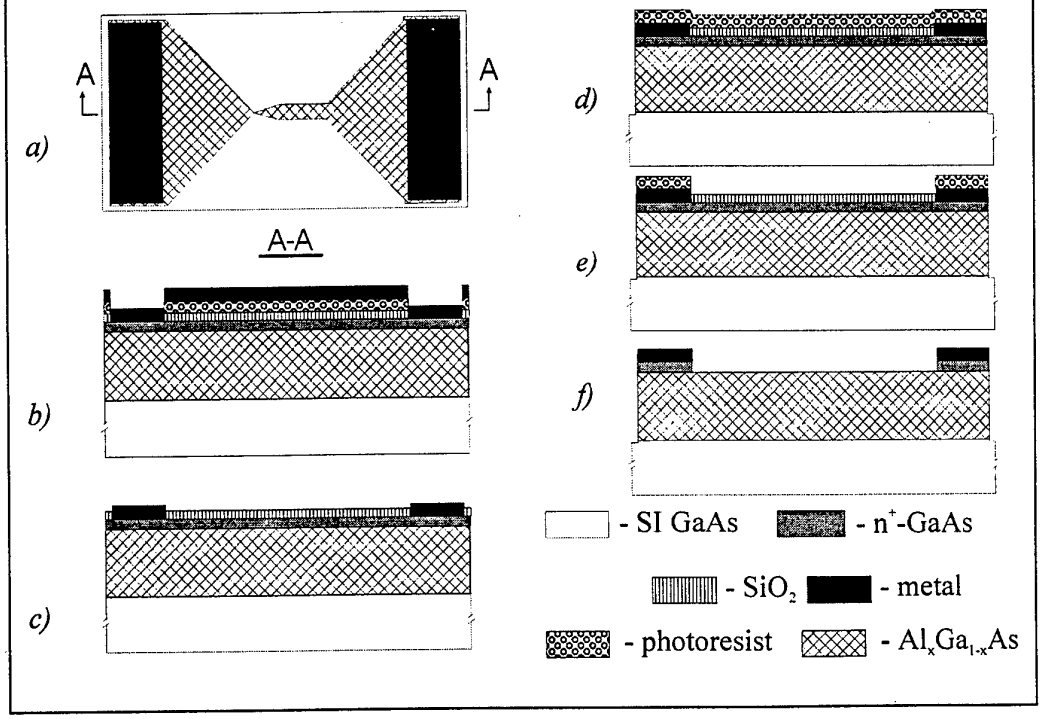

contacts was also different: cooper with vanadium substratum were evaporated thermally onto aluminum.

The fabrication process of barrier-less asymmetrically shaped planar diode on the base of *n*-type AlGaAs epitaxial structure is depicted in **Figure 7**: schematic view of the diode is shown in **Figure 7, *a***, while the cross-section of the diode can be seen in **Figure 7, *f***. SiO_2 film of 0.2 μm thickness was plasma-chemically grown onto polished and chemically cleaned surface of the epitaxial structure. First photolithography step opened windows in SiO_2 film, and Ge/Ni/Au metals were thermally evaporated (**Figure 7, *b***). Annealing of the evaporated metals at $T = 425°C$ in Ar atmosphere created ohmic contacts for the diode (**Figure 7, *c***). The second photolithography step prepared pattern for mesa formation of the ASPD. After removing of SiO_2 in the opened windows, the epitaxial n^+-GaAs and *n*-AlGaAs layers were etched in $H_2SO_4 : H_2O_2 : H_2O = 3:1:1$ solution. **Figure 7, *d*** represents deep mesa formation in the diode when the epitaxial layers were etched through up to the semiinsulating substrate. In the case of shallow mesa, the etching depth fell into the range of (10÷15) μm. The third photolithography step was performed to protect ohmic contacts during chemical removing of the conductive n^+-GaAs layer (**Figure 7, *e***) which was etched in $H_2SO_4 : H_2O_2 : H_2O = 8:1:1$ solution (**Figure 7, *f***).

The wafers with ASPD array were sliced into separate diode units, and then Au wires were bonded to each metallic ohmic contact by thermo-compression technique. The diodes were mounted into a universal rectangular waveguide head [2]. In the case of microwave measurements in a X-frequency range the waveguide head represented a lowered waveguide section: the distance between the wide walls in the window was equal 3.4 mm. For a K_a-frequency range measurements a universal non-lowered

waveguide head with its $3.4 \times 7.2\ mm^2$-window was used. Experiments were performed using microwave generators operating at $f = 10$ GHz and $f = 35$ GHz frequencies [2]. The microwave signals were modulated by rectangular pulses produced by a pulse generator: duration of the pulse ranged from tenth to several units of microseconds. Low repetition rate of the microwave pulses ($f_{pulse} = 40$Hz) was chosen to avoid crystal lattice heating of the diodes.

Experimental Results

Electrical resistance of the asymmetrically shaped planar diodes was measured in dc regime, while electrical capacitance of the diodes was measured at 1 MHz frequency. Table 3 summarizes the electrical parameters of various ASPD. The value of electrical resistance of the ASPD produced on the base of silicon single-crystal was mainly determined by the electrical resistance of the substrate. In the case of the ASPD on the base of AlGaAs epitaxial layer the resistance was determined by the geometrical parameters of the configured semiconductor layer. Electrical capacitance of the diodes was conditioned by the diffusion capacity of the semiconductor. It is worth to note the decrease of the time constant $\tau = RC$ of the diodes with increasing electrical resistivity of the semiconductor. The most prospective microwave detector for high operational speed application turned to be the ASPD on the base of *p*-type Si (resistivity 40 Ω·cm), i.e. these detectors could be used to detect microwave pulses of nanosecond duration. The microwave diodes on the base of semiconductors of lower resistivity could detect microwave pulses of the duration of several tens of nanoseconds. Higher values of the time constant were inherent to the ASPDs fabricated on the base of AlGaAs epitaxial layer and were independent of AlAs mole fraction *x*. The slowest microwave detectors, as seen from the results presented in **Table 3**, were the ASPDs additionally shunted by n^+-layer on the bottom of the semiconductor substrate. Substantial increase of the electrical capacity of the diode determined high values of the time constant τ, despite the essential decrease of their electrical resistance.

Table 3. Electrical parameters of various ASPD

Diode	Material	*R*, Ω	*C*, pF	τ, ns
with *l-h*	*n*-Si, 5 Ω·cm	120÷190	50÷140	10÷16
with *l-h*	*p*-Si, 4.5 Ω·cm	155÷165	50÷70	9÷11
with *l-h*	*p*-Si, 10 Ω·cm	270÷300	20÷25	6÷6.5
with *l-h*	*p*-Si, 40 Ω·cm	700÷1400	0.7÷2.5	1.0÷1.5
with *l-h*, shunted by n^+ bottom layer	*n*-Si, 5 Ω·cm	30÷50	1000÷2500	30÷70
barrier-less, shunted by n^+ bottom layer	*n*-Si, 5 Ω·cm	40÷50	500÷1500	30÷50
barrier-less	*n*-Si, 5 Ω·cm	275÷325	15÷25	5.5÷6.5
barrier-less	*n*-$Al_{0.19}Ga_{0.81}As$, 0.05 Ω·cm	90÷100	200÷250	20÷25
barrier-less	*n*-$Al_{0.23}Ga_{0.77}As$, 0.5 Ω·cm	2000÷3000	5÷12	20÷30
barrier-less	*n*-$Al_{0.31}Ga_{0.69}As$, 2.5 Ω·cm	11000÷20000	1.0÷2.0	10÷25

Linear character of current-voltage characteristic was inherent to all types of the ASPDs at low applied voltages. Meanwhile, at higher voltage values the I-V characteristics became sublinear due to charge carrier heating in strong electric field. The asymmetry of the I-V characteristics of the ASPD with *l-h* junction corresponded to the geometrical configuration: forward direction of the electric current was set for the case when the highly doped region of the diode close to the "neck" was biased negative for *n*-type diodes, and on the contrary, positive for the ASPD fabricated from *p*-type semiconductor. In the case of the asymmetrically shaped barrier-less diodes the asymmetry of the I-V characteristics had opposite sign: the forward current took place when the more-necked side of the diode was biased positive for *n*-type semiconductor and negative for *p*-type of conductivity.

Microwave experiments revealed the correspondence between the detected voltage polarity and the sign of the I-V characteristics asymmetry of the ASPD. When the diode was fabricated on the base of n-n^+ junction, negative detected voltage was measured with respect to the grounded n^+ part of the diode. **Figure 8** depicts the dependence of the detected voltage U_d on incident microwave power P_i for several types of the ASPDs with n-n^+-Si junction ($\rho = 5\ \Omega\cdot$cm) measured at $f = 10$ GHz frequency. Linear character of the presented voltage-power characteristics was inherent for all types of the ASPDs, however their dynamic range was different. The narrowest dynamic range was observed in the case of the ASPD additionally shunted by n^+ layer arranged on the bottom of the pad of the diode. Lower limit of the dynamic range of this diode was set by low voltage sensitivity, while puny upper limit was set by high value of the electrical capacitance of the ASPD (see Table 3). The

Figure 8. Voltage-power characteristics of ASPDs with n-n^+ junction on the base of *n*-type Si single-crystal. Microwave frequency $f = 10$ GHz.

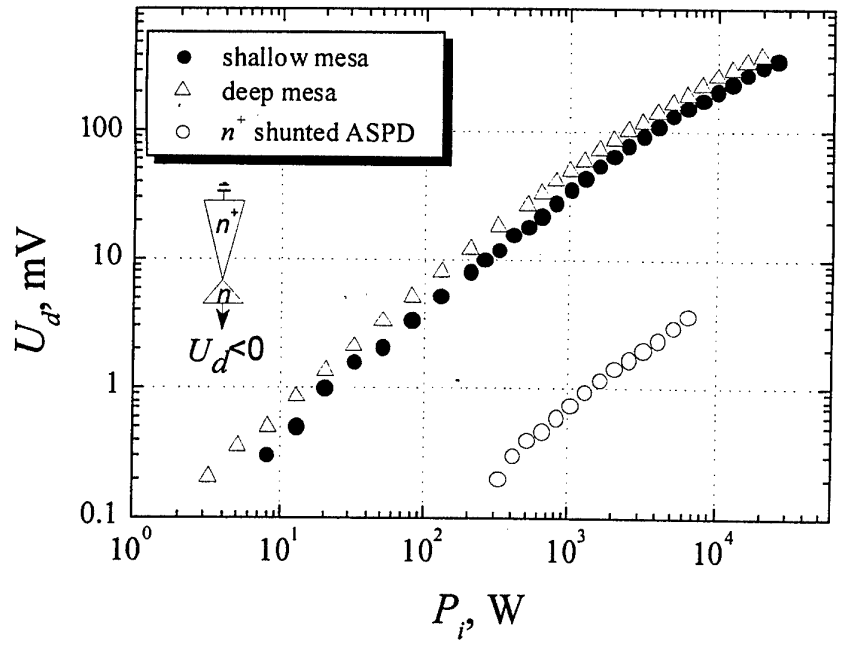

presence of high capacitance not only lowered the operational speed of the diode but also was critical in high power region: at a certain value of microwave power the breakdown processes in the diode began, and therefore abrupt decrease of the detected voltage was observed instead of gradual deflection from the linear law, like it was for the not shunted ASPDs. There was no substantial difference between the detection properties of the ASPD having shallow ($h_{mesa} = 5$ μm) and deep ($h_{mesa} = 10$ μm) mesas. Comparison of experimental values of the voltage sensitivity in respect of incident power with theoretical values of the voltage sensitivity in respect of absorbed power (see **Figure 1, *a***) gave the factor indicating the relative part of the absorbed microwave power to be equal to $(0.7 \div 1.4) \times 10^{-5}$. Taking the value $K = 1 \times 10^{-5}$ the upper limit of dynamical range of the ASPD with *l-h* junction was calculated and presented in **Figure 2, *a***. Higher value of the upper dynamic range limit in the shallow-mesa case (**Figure 8**) seems to be contradictory to the theoretical dependence of the limit on the mesa depth. However, the latter dependence was calculated using the same value of the K factor, while it had to be higher for the deeper mesa and, thus, the theoretical upper limit had to be lower than presented in **Figure 2, *a***.

In the case of asymmetrically shaped barrier-less *n*-type silicon the sign of the detected voltage was opposite to that of the ASPD with n-n^+ junction. The voltage-power characteristics of the barrier-less diodes are presented in **Figure 9**. Just like for the ASPD with n-n^+ junction, additional shunting of the diode essentially suppressed its dynamic range due to lower voltage sensitivity and greater electrical capacitance. In contrast to the ASPD with *l-h* junction, now significant difference in the voltage sensitivities for the shallow and deep mesas should be noted. The explanation of this experimental fact lies in specific mechanism of microwave radiation detection in homogeneous asymmetrically shaped semiconductor structure, when the detected

Figure 9. Voltage-power characteristics of barrier-less ASPD on the base of *n*- Si single-crystal. Microwave frequency $f = 10$ GHz.

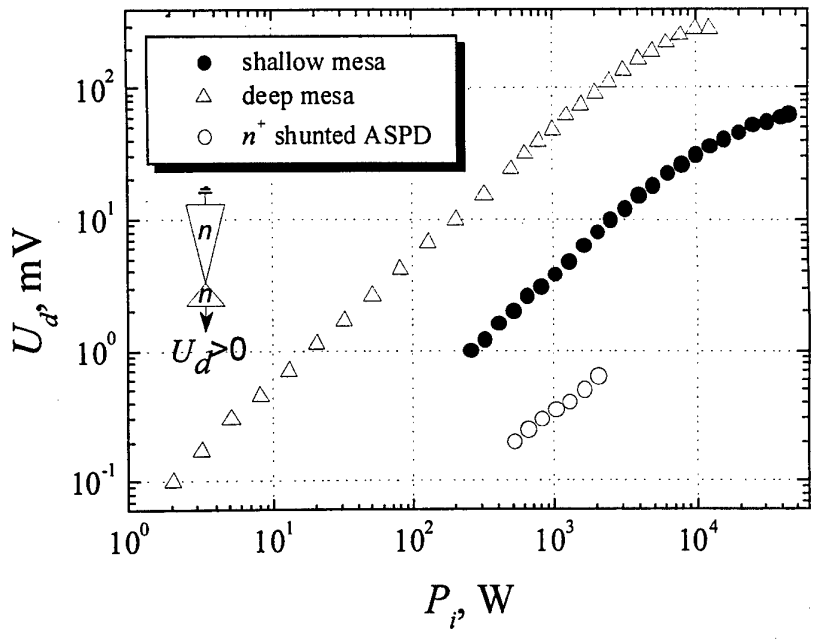

voltage depended more on the geometrical shape of the structure than on its doping character like it was in the case of the ASPD with *l-h* junction. In addition, the factor K was higher for the barrier-less diode with deeper mesa than for the shallow mesa case because of the substantial difference in the values of electrical resistance of the structures. This circumstance explains also at first sight strangely looking disagreement between experimental and theoretical estimations of the upper limit of the dynamic range. The dependence of the limit on mesa depth (see **Figure 2, *b***) was calculated taking $K = 1\times10^{-5}$, i.e. having constant value, while it had to be taken higher for the deeper mesa cases. Finally, one more reason of stronger dependence of the barrier-less diodes' voltage sensitivity on mesa depth could be mentioned: pure bigradient electromotive force arises when the material is highly homogeneous and electrical connection to the semiconductor is performed over high quality ohmic contacts. If not a case, under the radiation secondary mechanisms of microwave detection can induce additional *emfs* which can govern the total value of the measured voltage, especially if the bigradient effect is not strong enough. That is why the requirements for semiconductor material and for processing of the barrier-less ASPD must be higher than those for the microwave diodes with *l-h* junction. Nevertheless, the use of the barrier-less diodes in HPM application seems to be more promising, as it is evident from the experimental data in **Figure 9** and theoretical estimations in **Figure 2, *b***.

Figure 10 shows voltage-power characteristics of the ASPDs on the base of *n*-type Si, when the diodes were exposed to microwave radiation of 10 GHz and 35 GHz frequencies. Stronger dependence of the voltage sensitivity on frequency was observed for the *n-n*$^+$ ASPD with shallow mesa: the voltage sensitivity at 35 GHz was higher than that at 10 GHz frequency. In other cases, i.e. for the *n-n*$^+$ ASPD with deep

Figure 10. Voltage-power characteristics of ASPD on the base of single-crystal *n*- Si at $f = 10$ GHz and $f = 35$ GHz microwave frequencies.

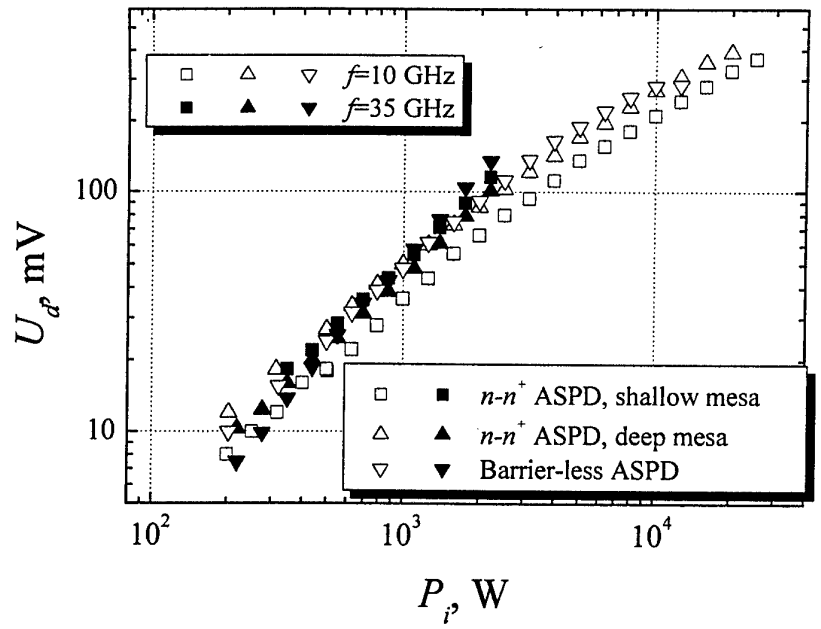

mesa and for the barrier-less microwave diode, no significant frequency dependence was observed. However, the voltage-power characteristic of the barrier-less ASPD was slightly supper-linear at $f = 35$ GHz. This nonlinearity could be explained taking into account additional detection mechanisms beside the bigradient effect of hot carriers.

Polarity of the voltage detected on the ASPD with p-p^+ junction corresponded to that inherent to thermoelectric *emf* of hot carriers, i.e. positive voltage was measured with respect to grounded p^+ part of the microwave diode (see inset in **Figure 11**). Irrespective of electrical resistivity ρ, the signal induced on p-Si ASPDs linearly depended on incident microwave power of low values, as can be seen in **Figure 11**. However, the upper dynamic range limit of the investigated diodes was different. The voltage-power characteristic of the ASPD on the base of lower electrical resistivity ($\rho = 4.5$ Ω·cm) was linear in the whole range of microwave power measured. High upper limit of the dynamic range can be explained by low absorption value ($K \approx 7 \times 10^{-7}$), that follows from the comparison of experimental voltage sensitivity $S_i = 1$ mV/kW, derived according to results in **Figure 11**, and calculated voltage sensitivity with respect to absorbed microwave power $S_a = 1.5$ V/W (see **Figure 1, *a***). The increase of electrical resistivity of the initial semiconductor on the base of which the p-p^+-Si ASPDs were fabricated suppressed the upper limit of their dynamic range. Good correspondence between the experimental limit of dynamic range and the calculated one could be noticed (see **Figure 2, *a***).

Investigations of microwave detection in asymmetrically shaped barrier-less $Al_xGa_{1-x}As$ epitaxial layers revealed the variety of features inherent to this type of the ASPD. **Figure 12** depicts the voltage-power characteristics of the diodes the detection

Figure 11. Voltage-power characteristics of ASPD with p-p^+ junction on the base of p-type Si single-crystal. Microwave frequency $f = 10$ GHz.

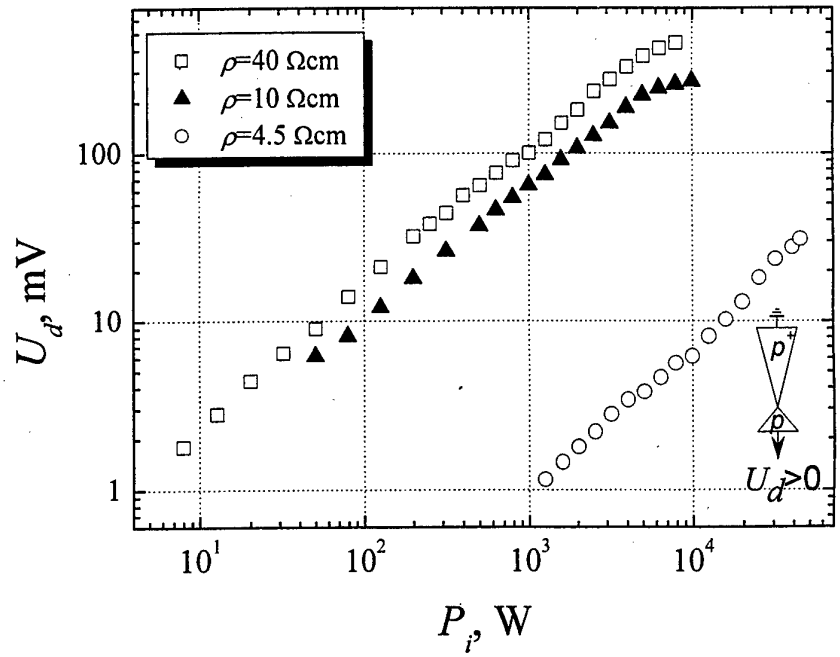

Figure 12. Voltage-power characteristics of barrier-less ASPD on the base of *n*-type $Al_xGa_{1-x}As$. Microwave frequency $f = 10$ GHz.

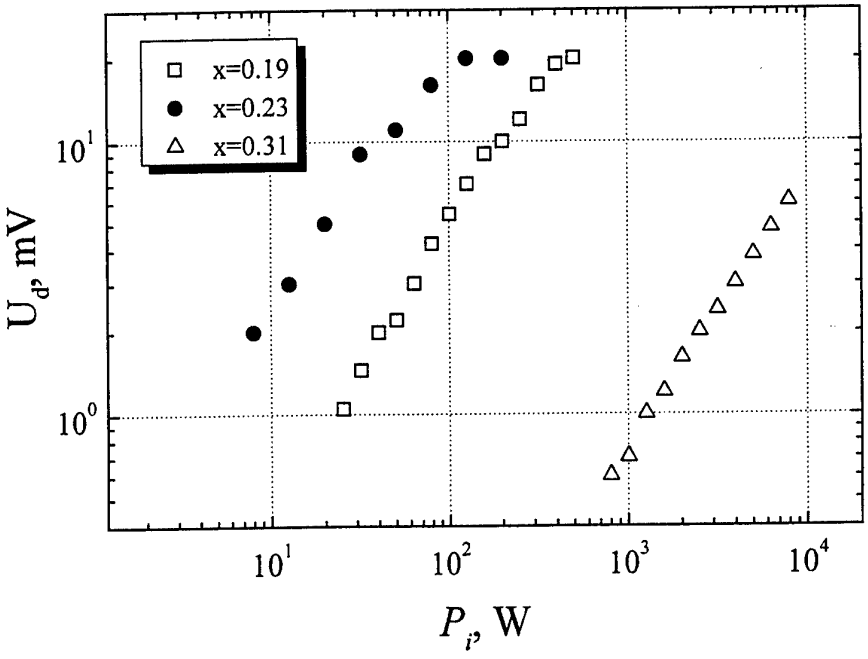

properties of which can be explained by the hot carrier bigradient effect. Namely, the polarity of the detected voltage corresponded to that of the bigradient *emf*: in the case of grounded more-necked part of the diode the positive voltage pulse was measured. Note, that the voltage sensitivity non-monotonically depended on AlAs mole fraction x: the highest voltage sensitivity was measured for the diodes with $x = 0.23$, while the lowest one was observed in the case of $x = 0.31$. Substantial decrease of carrier concentration accompanied by slight decrease of electron mobility in $Al_{0.23}Ga_{0.77}As$ layer compared with those in $Al_{0.19}Ga_{0.81}As$ enabled more effective separation of electric charge and, as a result, more effective rise of the electromotive force in the asymmetrically shaped semiconductor structure. However, further decrease of the carrier density was accompanied by significant decrease of electron mobility, what in turn worsened the conditions for the bigradient *emf* to originate. On the other hand, substantial increase of the semiconductor electrical resistivity lowered the portion of microwave power that could be absorbed by the diode. This consideration explains the increase of the upper dynamic range limit of the diode on the base of *n*-type $Al_{0.31}Ga_{0.69}As$. Low values of the upper dynamic range limit of the diodes on the base of $Al_xGa_{1-x}As$ with $x = 0.19$ and $x = 0.23$ were caused by the change of the detected voltage polarity at higher microwave powers. Moreover, for ASPDs fabricated on the base of $Al_{0.31}Ga_{0.69}As$, in some cases the polarity of the detected voltage was opposite to that of the bigradient *emf*.

In order to realize the situation, photoluminescence spectra of $Al_xGa_{1-x}As$ layers excited by Ar-laser light were investigated by a single photon counting method. These dependences explored at liquid nitrogen temperature are shown in **Figure 13**. Excitonic photoluminescence peaks $[DX]_\Gamma$ corresponded to the forbidden energy gap of $Al_xGa_{1-x}As$ with x equal to 0.19, 0.23 and 0.31. Additional peaks were observed for

Figure 13. Photoluminescence spectra of *n*-type $Al_xGa_{1-x}As$ layers having different *x* values. *T* = 77 K.

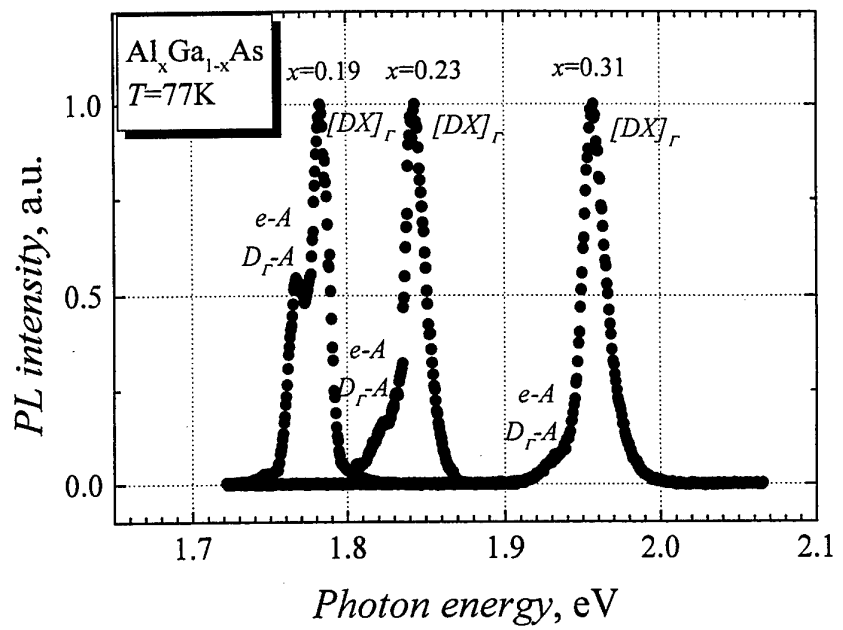

all the investigated materials, however, their prominence vanished with the increase of *x* value. These additional peaks we associate with electron transition from conductivity band edge to acceptor level (*e-A*) and from donor level to acceptor (D_Γ-*A*). The value of energy difference between the $[DX]_\Gamma$ and *e-A* / D_Γ-*A* peaks (20÷30 meV) allowed us to identify the acceptor level of carbon impurity C_{As}. As AlAs mole fraction increased, the additional photoluminescence peak intensity decreased, what could be explained by increasing population of impurity levels with electrons. Presence of compensating acceptor impurities in *n*-type $Al_xGa_{1-x}As$ not only reduced the electron mobility but also capacitated the formation of charge inhomogeneity in the material. That is why the microwaves were detected not only in the asymmetrically shaped semiconductor structure but also on the charge inhomogeneities. If the detected voltage had opposite sign than that of the bigradient *emf*, then the resultant detected signal decreased and even changed its sign, thus reducing the upper limit of dynamic range of the ASPD on the base of *n*-type $Al_xGa_{1-x}As$.

Figure 14 depicts the dependences of the detected voltage having the polarity opposite to that of the voltage shown in **Figure 12.** The voltage detected on the diodes fabricated on the base of $Al_xGa_{1-x}As$ with $x = 0.19$ and $x = 0.23$ changed its polarity with increasing microwave power. We associate this voltage with the microwave detection on charge inhomogeneities of semiconductor material. Very narrow dynamic range of the voltage-power characteristic was inherent to these ASPDs in the region of inverted polarity. Lower limit of the dynamic range in the inverted polarity region was determined by the competition of two detection mechanisms, namely, of

Figure 14. Voltage-power characteristics of barrier-less ASPD on the base of inhomogeneous *n*-type $Al_xGa_{1-x}As$. Microwave frequency f = 10 GHz.

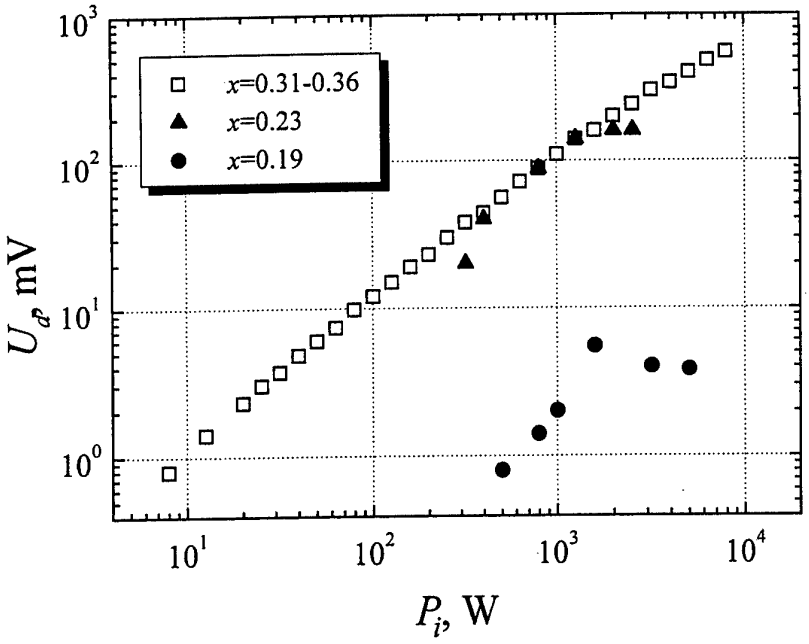

the bigradient *emf* and of the detection on charge inhomogeneities. The upper limit of the dynamic range is associated with breakdown processes occurring in inhomogeneous semiconductor.

Different character of the voltage-power characteristic was observed on the ASPD samples on the base of $Al_xGa_{1-x}As$ with $x = 0.31 \div 0.36$ (see **Figure 14**). Here, the polarity of the detected voltage was opposite to that of bigradient *emf* in the entire range of applied microwave power and the voltage-power characteristic was linear almost up to 10 kW. Photoluminescence data of these samples are presented in **Figure 15.** Two photoluminescence spikes could be distinguished for different values of AlAs mole fraction $x = 0.31$ and $x = 0.36$. This implies the semiconductor material to be of a polycrystalline nature. The presence of the semiconductor regions with different x in the ASPD may determine the inter-grain detection mechanism of the diode. However, on the contrary to the asymmetrically shaped semiconductor structures on the base of $Al_xGa_{1-x}As$ with smaller x values, the ASPD on the base of polycrystalline semiconductor can be used in HPM application.

Figure 15. Photoluminescence spectra of inhomogeneous *n*-type $Al_xGa_{1-x}As$ at $T = 77$ K.

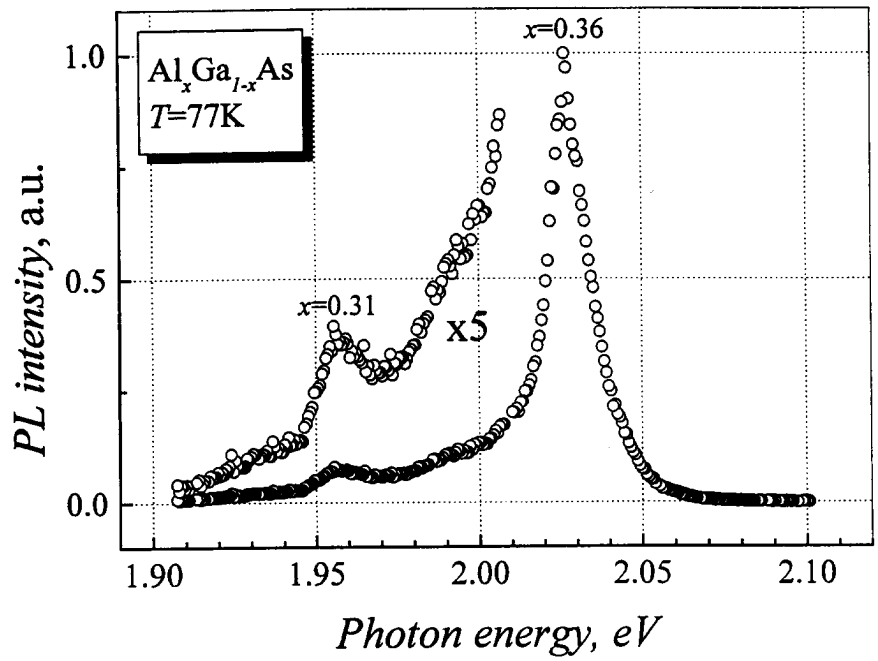

Conclusions

Both theoretical and experimental investigations of asymmetrically shaped semiconductor structures on the shunting pad of the same semiconductor allowed us to arrive at the following conclusions.

Phenomenological theory of charge carrier transport through asymmetrically shaped *l-h* junction in microwave electric field predicts that:

- The detectors on the base of asymmetrically shaped p-p^+ junction on a single crystal silicon with electrical resistivity (4.5÷10) Ω·cm and on the base of the asymmetrically shaped n-n^+ junction of $Al_{0.4}Ga_{0.6}As$ are the best candidates for wide frequency band applications having frequency-independent range of voltage sensitivity from gigahertzs to terahertzs.
- Upper dynamic range of the microwave diodes on the base of asymmetrically shaped p-p^+ junction and on the base of homogeneous asymmetrically configured p-type Si of low electrical resistivity can reach the value of 100 kW.

Experimental investigations can be summarized in the following propositions:

- Higher operational speed is inherent to the asymmetrically shaped planar microwave diodes fabricated on the base of higher resistivity semiconductor; for example, the time constant of the ASPDs on the base of p-type Si with $\rho = (10 \div 40)$ Ω·cm has the value of several nanoseconds.
- Dynamic range of the asymmetrically shaped barrier-less microwave diodes on the base of n-type Si is wider than that of the diodes with asymmetrically configured n-n^+ junction, and it can reach 10 kW limit for shallow mesa case. The upper limit of the dynamic range is higher for the diodes with more shallow mesas.
- Weak frequency dependence of voltage sensitivity is specific both for the barrier-less microwave diodes and the diodes with asymmetrically shaped n-n^+ junction. The voltage sensitivity values of both types of the ASPD fall in the range of (35÷50) mV/kW at 10 GHz and 35 GHz microwave frequencies.
- The best value of the upper dynamic range limit, 40 kW, is reached for the microwave diodes with asymmetrically shaped p-p^+ junction of p-type Si having electrical resistivity $\rho = 4.5$ Ω·cm. This is achieved due to effective shunting of microwave currents by the semiconductor substrate and higher value of critical electric field strength E_c for the p-type silicon.
- In contrast to the expectations, the highest value of the upper dynamic range limit (~10 kW) for the barrier-less ASPDs configured on n-type $Al_xGa_{1-x}As$ is achieved in the case of AlAs mole fraction $x = 0.31$. Non-monotonic character of voltage-power characteristic is inherent to the barrier-less diodes with lower x values; this can be explained by the existence of electrical charge inhomogeneities in the semiconductor structure.
- Polycrystalline nature of the $Al_xGa_{1-x}As$ layers with higher value of AlAs mole fraction is responsible for the opposite polarity of the detected voltage. This feature of the ASPD can be employed for high power microwave measurements.

Recommendations

Difficulties interfering with presentable implementation of theoretically grounded proposition stating that in high power microwave applications the barrier-less diode takes precedence over the diode on the base of asymmetrically shaped *l-h* junction, are mainly lying in a problem of semiconductor material homogeneity. Another reason limiting successful use of the barrier-less diodes is microwave detection on non-linearity of metallic contacts to the diodes. This drawback raises hard requirements for the quality of the ohmic contacts. Accordingly, some recommendations how to purify the bigradient phenomenon in the barrier-less asymmetrically shaped semiconductor structure are presented hereunder:

- Accurate selection of semiconductor wafers must be performed before starting fabrication process of the microwave diode, and special attention should be paid to the plane homogeneity of the semiconductor material. Crystalline quality of $Al_xGa_{1-x}As$ epitaxial layers grown by liquid phase epitaxy should be controlled.
- Measures ensuring both low resistivity and linearity of the metal contacts to the microwave diode must be taken.
- The design of the asymmetrically shaped planar microwave diode should be changed with intent to minimize or even avoid exposition of the metallic contacts to microwave radiation.

References

1. Steponas Ašmontas and Algirdas Sužiedėlis. "Hot electron thermoelectricity". Journal of Thermoelectricity, N 1, pp. 5-26 (1997).
2. S.Ašmontas, A.Sužiedėlis, "Detection of wide frequency band microwave signals in ultra-wide dynamic range using a barrier-less semiconductor diode", Final report on the Special contract SPC 00-4057, F61775-00-WE057, 2001.
3. S. Ašmontas, J. Gradauskas, J. Kundrotas, A. Sužiedėlis, A. Šilėnas, and G. Valušis, "New aspects of microwave detection in GaAs/AlGaAs heterojunctions", in: *Proc. 24th Int. Conf. on Physics of Semiconductors 24ICPS'98*, Jerusalem, Israel, Aug. 3-9, 1998, D.Gershoni, Ed., CD-ROM (1193.pdf) (World Scientific) 1999.
4. S.Ašmontas, A.Sužiedėlis, "Fast detection of high power microwave signals using asymmetrically shaped semiconductor structures", Performance Report on Award No. FA8655-03-3021, 2003.

Acknowledgements

The material presented in this report is based upon work supported by the European Office of Aerospace Research and Development, Air Force Office of Scientific Research, Air Force Research Laboratory under Contract No. FA8655-03-1-3021. Any opinions, findings and conclusions or recommendations expressed in this material are those of the authors and do not necessarily reflect the views of the European Office of Aerospace Research and Development, Air Force Office of Scientific Research, Air Force Research Laboratory.

Clause Statements

(1) In accordance with Defense Federal Acquisition Regulation 252.227-7036, Declaration of Technical Data Conformity (Jan 1997),

The Contractor, *STEPONAS AŠMONTAS,* hereby delcares that, to the best of its knowledge and belief, the technical data delivered herewith under Contract No. FA8655-03-1-3021 is complete, accurate, and complies with all requirements of the contract.

DATE: 16/03/2004

Name and Title of Authorized Official: S. Ašmontas
Director of Semiconductor Physics Institute

(2) In accordance with the requirements in Federal Aquisition Regulation 52.227-13, Patent Rights—Acquisition by the *U.S.* Government (Jun 1989),

"I certify that there were no subject inventions to declare as defined in FAR 52.227-13, during the performance of this contract."

DATE: 16/03/2004

Name and Title of Authorized Official: S. Ašmontas
Director of Semiconductor Physics Institute

Appendix A

Table A1. Positive and negative features of different methods for microwave power measurement

Method of microwave power measurement	Positive																Negative															
	High accuracy	Compact	Use of low power meters	Simplicity	Reliability	Possibility measure pulse and CW signals	High power	Wide dynamic range	Independence on temperature, humidity	Economy	High operational speed	Hardiness against overload	Wide frequency range	Frequency selectivity	Independence of harmonics	Necessity of calibration	Problems with power attenuation	Low frequency	Low accuracy	Dependence on harmonics	Additional correction of measurement results	Inertia of measurements	Bulky equipment	Dependence on frequency	Low sensitivity	Complicated maintenance	Sensitivity to mechanical effect	Sophisticated fabrication	Narrow frequency range	Low power	Dependence on temperature	Narrow dynamic range
Power attenuation method	+	+	+													+	+															
Transducer on the base of vacuum diodes				+	+	+												+	+	+	+											
Calorimetric method	+						+	+														+	+									
Directional coupler method				+					+									+	+										+			
Semiconductor thermocouple				+	+		+		+							+			+					+								
Absorptive waveguide wall method				+	+														+			+			+	+						
Pondemotoric method				+						+	+	+															+	+	+				
Hall effect method	+										+																			+	+	
Magnetoresistance method						+					+		+						+											+		
Nonlinear ferrite converter					+	+	+							+																		+
Semiconductor resistance change				+							+				+									+	+						+	+
Hot carrier thermo emf method				+	+		+				+				+	+															+	+